

Divergent Synthesis of 48 Heparan Sulfate-Based Disaccharides and Probing the Specific Sugar–Fibroblast Growth Factor-1 Interaction

Yu-Peng Hu,^{†,‡,§,¶} Yong-Qing Zhong,^{†,‡,§,¶} Zhi-Geng Chen,^{†,‡,§,¶} Chun-Yen Chen,[‡] Zhonghao Shi,[†] Medel Manuel L. Zulueta,[†] Chiao-Chu Ku,[§] Pei-Ying Lee,[†] Cheng-Chung Wang,^{‡,§} and Shang-Cheng Hung^{*,†,||}

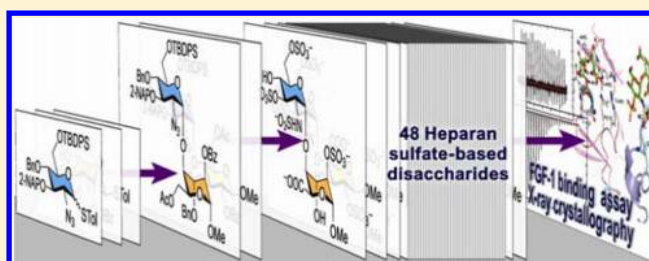
[†]Genomics Research Center and [§]Institute of Chemistry, Academia Sinica, 128, Section 2, Academia Road, Taipei 115, Taiwan

[‡]Department of Chemistry, National Tsing Hua University, 101, Section 2, Kuang-Fu Road, Hsinchu 300, Taiwan

^{||}Department of Applied Chemistry, National Chiao Tung University, 1001, Ta-Hsueh Road, Hsinchu 300, Taiwan

Supporting Information

ABSTRACT: Several biological processes involve glycans, yet understanding their ligand specificities is impeded by their inherent diversity and difficult acquisition. Generating broad synthetic sugar libraries for bioevaluations is a powerful tool in unraveling glycan structural information. In the case of the widely distributed heparan sulfate (HS), however, the 48 theoretical possibilities for its repeating disaccharide call for synthetic approaches that should minimize the effort in an undoubtedly huge undertaking. Here we employed a divergent strategy to afford all 48 HS-based disaccharides from just two orthogonally protected disaccharide precursors. Different combinations and sequence of transformation steps were applied with many downstream intermediates leading up to multiple target products. With the full disaccharide library in hand, affinity screening with fibroblast growth factor-1 (FGF-1) revealed that four of the synthetic sugars bind to FGF-1. The molecular details of the interaction were further clarified through X-ray analysis of the sugar–protein cocrystals. The capability of comprehensive sugar libraries in providing key insights in glycan–ligand interaction is, thus, highlighted.



INTRODUCTION

Glycans are exceptionally diverse and complex that deciphering the functions embedded within the glycome is a substantial challenge.¹ The multiple regio- and stereochemical permutations in linking several monosaccharide units and the modifications that may follow chain assembly allowed these complex sugars to hold structural information densities surpassing DNA and proteins. With regulated rather than template-driven biosyntheses, their expression often produces an array of related structures that may possess subtle differences in activity. A case in point is heparan sulfate (HS), a proteoglycan sugar component with crucial roles in metazoan development, physiology, and disease as a dynamic regulator of protein activities at the cell–extracellular interface.² The modifications of the HS precursor, made up of an extended 1→4-linked *N*-acetyl- α -D-glucosamine (GlcNAc) and β -D-glucuronic acid (GlcA) copolymer, facilitated by several enzyme isoforms of varying specificities are always incomplete, resulting in extensive chain microheterogeneity.³ These modifications, which include GlcNAc *N*-deacetylation, GlcA 5-C-epimerization toward α -L-iduronic acid (IdoA), and sulfonations at 2-N, 3-O, and 6-O of α -D-glucosamine (GlcN) and at 2-O of the uronic acid, overall account for 48 theoretical possibilities for the repeating disaccharide (Figure 1). Consequent of being widespread in cell surfaces, extracellular matrices, and basement

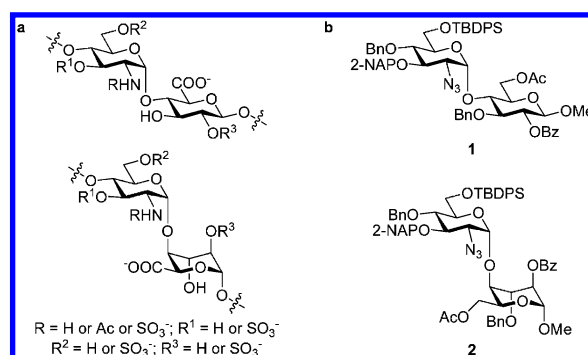


Figure 1. Structures of (a) the 48 disaccharides theoretically present in HS and (b) the orthogonally protected disaccharide precursors utilized in our divergent synthesis.

membranes, numerous proteins of various origins and functions evolved to associate with and take advantage of the elaborate patterns decorating the HS backbone.⁴ Recognizing the optimum patterns sought by binding proteins could guide the development of novel diagnostic agents and biomedical interventions. Under such premise, fondaparinux, a synthetic

Received: September 10, 2012

Published: December 14, 2012

pentasaccharide based on the HS analogue heparin, is now a clinically approved anticoagulant that is free of the main side effects of heparin therapy.⁵ Chemically defined materials are indispensable components of structure–activity relationship assays. Because sugar structures obtained from natural sources are generally unsuitable for these purposes, synthetic strategies have advanced to deliver these much needed compounds for biological studies.^{1,6}

Developing broad synthetic sugar libraries, aimed at probing the character of carbohydrate interactions with their ligands, is envisioned as a potent tool in understanding the fundamental roles of glycans in biological systems. For HS, the library should ideally include constructs covering the entire range of structures found within the polysaccharide. However, building such a collection is hampered by the number and diversity of compounds that have to be considered as well as the notorious technical difficulty of HS syntheses.^{6b,7} There were recent successes in preparing particular sequences using chemo-enzymatic methodologies,⁸ but reaction completion and monitoring, availability of chemically pure starting materials, and product purification remain pervasive concerns. To prepare HS-based compounds, we turned to chemical synthesis, which proved reliable in accessing well-defined HS oligosaccharides.⁷ HS synthesis, nevertheless, offers unique challenges, such as the acquisition of the rare L-ido derivatives, the regio- and stereocontrol of glycosidic bond formation, and the judicious selection and manipulation of protecting groups to match the intricate functional group pattern of the desired products.

Synthetic efforts reported in the literature typically employ explicitly designed oligosaccharide precursors to access the target HS oligosaccharides through a myriad of functional group transformations.⁹ Furthermore, generating a typical trisulfonated HS-based disaccharide takes about 20 reaction steps from common monosaccharide starting materials. As such, building a comprehensive HS-based sugar library, with each compound obtained from an individual multistep route, would be a huge undertaking. Thus, efficient strategies that minimize the number of steps, such as making full use of shared intermediates, should be explored. Accordingly, we developed an orthogonal protecting group strategy that permitted access to all 48 disaccharides theoretically present in HS from only two disaccharide precursors, one with a D-glucosyl (**1**) and another with an L-idosyl unit (**2**) (Figure 1). These compounds were then transformed following a divergent process, where many downstream intermediates were utilized to make more than one final product. Fibroblast growth factor-1 (FGF-1), a prototypical member of the FGF family, was chosen to demonstrate the effectiveness of our disaccharide library in defining binding specificity. Thus, binding affinity screening and, subsequently, X-ray cocrystal analysis were conducted, the results of which are disclosed herein.

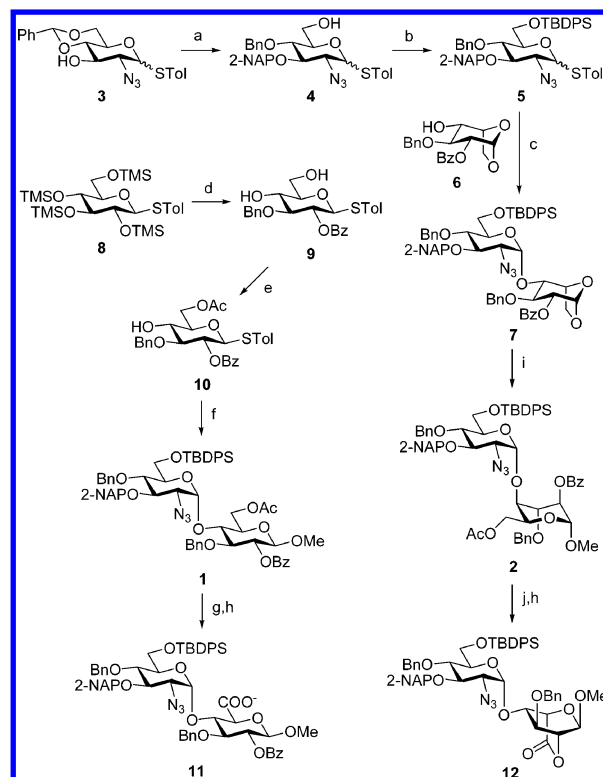
RESULTS AND DISCUSSION

Syntheses of 48 HS-Based Disaccharides. A carefully selected set of protecting groups was employed to decorate the disaccharide precursors **1** and **2**. We used the simple methyl group to block the anomeric position at the reducing end. Installations of the orthogonal benzoyl (Bz) group at the 2-O position of the D-glucosyl and L-idosyl units and 2-naphthylmethyl (2-NAP) and *tert*-butyldiphenylsilyl (TBDPS) groups at the respective 3-O and 6-O positions of GlcN cover the O-sulfonation patterns in HS. The 2-O-Bz group is also expected to confer neighboring group assistance during the

formation of the 1,2-*trans* glycosidic bond. Selective access to the primary alcohol for later oxidation to the carboxylate is provided by the acetyl (Ac) group. The amine was masked as an azide to take advantage of its nonparticipation in glycosylation, favoring the α -stereoselective glucosamylation via the anomeric effect. Moreover, the azide can be readily transformed into the amine, acetamide, or sulfamate in later synthetic steps. Finally, benzyl (Bn) groups are utilized to block the hydroxyls that would be free in the final compounds.

The disaccharide preparations started with Williamson etherification at 3-O of the thioglycoside **3**¹⁰ (93%) followed by borane-mediated reductive benzylidene 6-O-ring opening (97%) to obtain the 6-alcohol **4** (Scheme 1). The desired D-glucosaminy donor **5** was acquired in 90% yield after a typical 6-O-silylation procedure. Subsequent glycosylation of the known 1,6-anhydro-L-idopyranosyl 4-alcohol **6**^{9g} promoted by *N*-iodosuccinimide (NIS) and trimethylsilyl trifluoromethanesulfonate (TMSOTf) provided the α -disaccharide **7** in 64%

Scheme 1. Preparation of the Common Intermediates **11 and **12**^a**



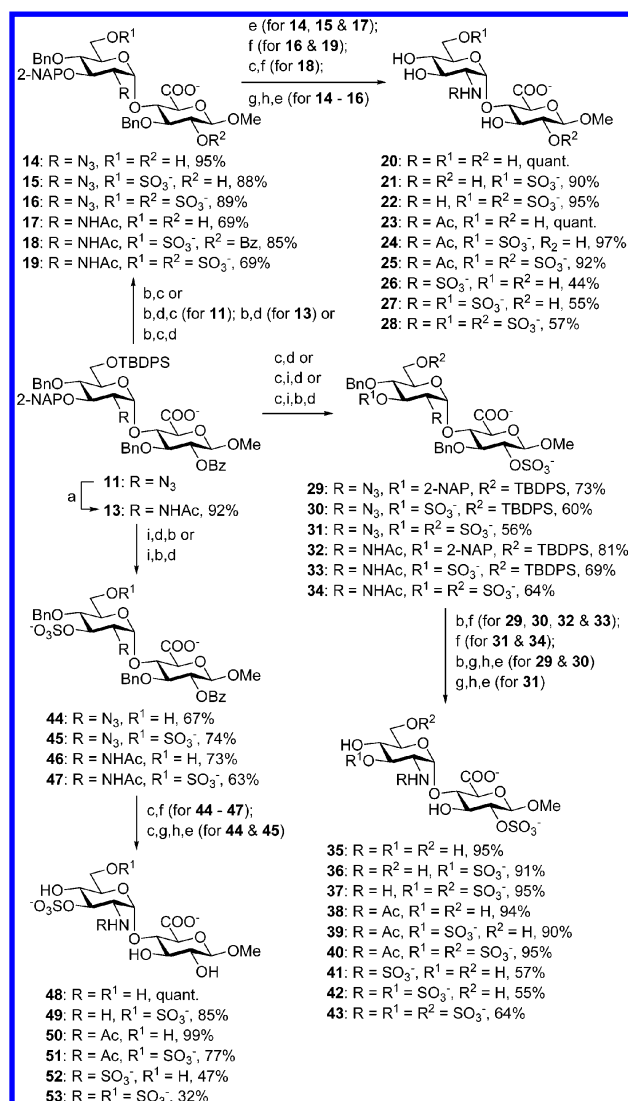
^aReagents and conditions: (a) (1) 2-NAPBr, NaH, DMF; 93%; (2) $\text{BH}_3 \cdot \text{THF}$, TMSOTf, CH_2Cl_2 , 0 °C, 6 h; 97%. (b) TBDPSCl, Et_3N , DMAP, CH_2Cl_2 , 0 °C to rt, 16 h; 90%. (c) NIS, TMSOTf, CH_2Cl_2 , 3 Å MS, -78 °C to rt, 2 h; 64%. (d) (1) benzaldehyde, TMSOTf, CH_2Cl_2 , 3 Å molecular sieves, 0 °C, 2 h; (2) benzaldehyde, TMSOTf, Et_3SiH , -78 °C, 4 h; (3) Bz_2O , TMSOTf, 0 °C, 18 h; (4) 70% $\text{TFA}_{(\text{aq})}$, 3 h, rt; 63% (4 steps, one pot). (e) Ac_2O , Et_3N , CH_2Cl_2 , 0 °C, 3 h; 86%. (f) (1) MeOH, NIS, TMSOTf, CH_2Cl_2 , 3 Å molecular sieves, -78 to -20 °C, 2 h; (2) **5**, TMSOTf, -78 to -20 °C, 3 h; 61% (2 steps, one pot). (g) $\text{Mg}(\text{OMe})_2$, CH_2Cl_2 , MeOH, 2 h; 93%. (h) TEMPO, BAIB, CH_2Cl_2 , H_2O , rt, 6 h; **11**, 90%; **12**, 89%. (i) (1) Ac_2O , $\text{Cu}(\text{OTf})_2$, 0 °C, 16 h; 91%; (2) saturated NH_3 , THF, MeOH, 0 °C, 3 h; 81%; (3) CCl_3CN , K_2CO_3 , rt, 16 h; 93%; (4) MeOH, AgOTf, CH_2Cl_2 , 3 Å molecular sieves, -5 °C, 1 h; 81%. (j) NaOMe, CH_2Cl_2 , MeOH, rt; 87%. DMAP: 4-(*N,N*-dimethylamino)pyridine.

yield together with the minor β -isomer (14%). Conversely, the regioselective one-pot protection¹¹ of the per-trimethylsilylated thioglucoside **8** furnished the corresponding 4,6-diol **9** in a 4-step yield of 63%. The transformations included the initial 4,6-O-benzylidene formation followed by silane-mediated regioselective 3-O-benylation, 2-O-benzoylation, and, last, acid hydrolysis of the benzylidene acetal. Exploiting the higher reactivity of the primary hydroxyl, the diol further underwent regioselective 6-O-acetylation to afford the 4-alcohol **10** (86%). Condensation of the acceptor–donor **10** with MeOH under NIS/TMSOTf promotion, followed in one pot by α -glycosylation with the thioglycoside **5** led to the fully protected precursor **1** in 61% yield. Mild deacetylation of the disaccharide **1** using $\text{Mg}(\text{OMe})_2$ ¹² (93%) and oxidation of the freed primary alcohol with catalytic 2,2,6,6-tetramethyl-1-piperidinyloxy free radical (TEMPO) in the presence of excess [bis(acetoxy)iodo]benzene (BAIB) delivered the carboxylate **11** (90%). Regarding the adduct **7**, acetolysis of the anhydro-ring was readily achieved in 91% yield using Ac_2O and copper(II) trifluoromethanesulfonate $[\text{Cu}(\text{OTf})_2]$.¹³ Treatment with saturated ammonia in a THF and MeOH cosolvent system enabled anomeric deacetylation (81%). Further trichloroacetimidate formation gave the glycosyl donor (93%), which was coupled with MeOH to acquire the target GlcN–IdoA precursor **2** in 81% yield. Successive Zemplén deacylation (87%) and TEMPO/BAIB oxidation (89%) finally produced the lactone **12**.

Compounds **11** and **12** were henceforth converted to the desired HS-based materials in a divergent manner through different combinations and sequence of transformation steps. Scheme 2 describes the syntheses of 24 disaccharides with GlcN–GlcA backbone. Thioacetic acid (AcSH)¹⁴ treatment of the disaccharide **11** accomplished the direct conversion of the azide to the acetamide to afford compound **13** in 92% yield. Both **11** and **13** were subjected to parallel reaction sequences toward the amino- and acetamido-containing final compounds. Tetra-*n*-butylammonium fluoride (TBAF) with equimolar AcOH, NaOMe in MeOH, and 2,3-dichloro-5,6-dicyano-1,4-benzoquinone (DDQ) were applied to chemoselectively cleave the TBDPS, Bz, and 2-NAP groups, respectively. Proper selection of these deprotection protocols exposed key hydroxyl groups for O-sulfonations, which are implemented using $\text{SO}_3\cdot\text{Et}_3\text{N}$ in DMF. To secure the sulfamate moiety, we first obtained the amine by reduction of the azide with 1,3-propanedithiol. N-Sulfonation was then carried out using $\text{SO}_3\cdot\text{Pyr}$ in the presence of NaOH and Et_3N . In the final step, palladium-catalyzed hydrogenolysis cleaved all arylmethyl (Bn and 2-NAP) ethers and, simultaneously, reduced the azido group to the free amine.

The acetamide **54** was similarly obtained using AcSH from compound **12** in 87% yield (Scheme 3). Unfortunately, the labile lactone in compounds **12** and **54** prompted a reconsideration of the desilylation reagent. The basic nature of TBAF promoted lactone hydrolysis (even with AcOH as coreagent), a result that we exploited in revealing the 2- and 6'-hydroxyls in one step. To spare the lactone function, removal of the TBDPS group was accomplished by treatment with the mild tris(dimethyl-amino)sulfonium difluorotrimethylsilicate (TASF).¹⁵ Lactone ring opening was separately achieved by LiOH. In an alternative but equally effective N-sulfonation procedure, the afforded amine, after global hydrogenolysis, was treated with $\text{SO}_3\cdot\text{Pyr}$ in basic (pH 9.5) aqueous conditions. Consequently and together with applicable reactions described

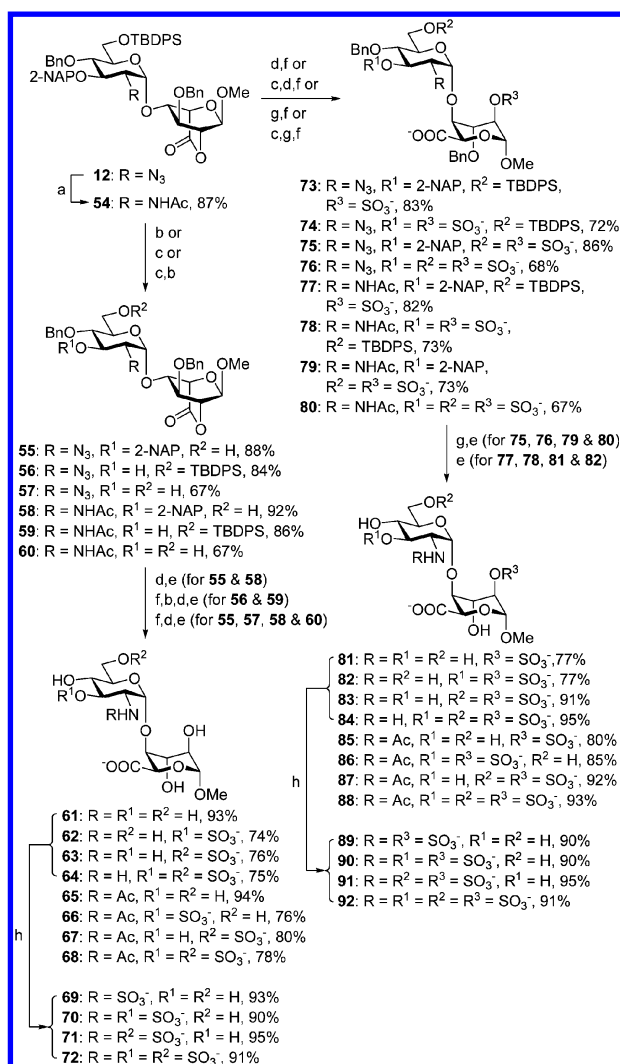
Scheme 2. Preparations of 24 HS-Based Disaccharides With GlcN–GlcA Backbone^a



^aReagents and conditions: (a) AcSH, Pyr, CH₂Cl₂, rt, 18 h. (b) TBAF, AcOH, 40 °C. (c) NaOMe, CH₂Cl₂, MeOH, rt. (d) $\text{SO}_3\cdot\text{Et}_3\text{N}$, DMF, 60 °C, 3 d. (e) $\text{Pd}(\text{OH})_2/\text{C}$, H₂ (balloon), phosphate buffer (pH 7), rt, 2 d. (f) Pd/C, H₂ (50 psi), MeOH, H₂O, rt, 2 d. (g) 1,3-propanedithiol, Et₃N, Pyr, H₂O, 50 °C. (h) $\text{SO}_3\cdot\text{Pyr}$, NaOH, Et₃N, MeOH, rt. (i) DDQ, CH₂Cl₂, H₂O, rt, 4 h. Pyr: pyridine.

for the GlcN–GlcA series, we acquired the other 24 disaccharides having the GlcN–IdoA structure. Thus, our target 48 HS-based disaccharides were generated from the intermediates **11** and **12** in 3–7 steps and 24–95% overall yields. Nuclear magnetic resonance and mass spectroscopic analyses confirmed the final product structures (see the Supporting Information, SI). Throughout the above-mentioned transformations, we strategically utilized numerous intermediates to prepare multiple target products, effectively reducing the effort in an otherwise laborious synthetic endeavor.

Evaluation of the Sugar Structures that Associate with FGF-1. FGFs are signaling proteins that take part in diverse processes, such as morphogenesis, wound repair, and angiogenesis.¹⁶ They also possess oncogenic roles in many cancers due in part to their key influence in cell proliferation, differentiation, and survival. The long polyanionic structure of

Scheme 3. Preparation of 24 HS-Based Disaccharides With GlcN–IdoA Backbone^a

^aReagents and conditions: (a) AcSH, Pyr, CHCl₃, rt, 1.5 h. (b) TASF, DMF, rt. (c) DDQ, CH₂Cl₂, H₂O, rt, 4 h. (d) LiOH, THF, H₂O, rt, 1 h. (e) Pd(OH)₂/C, H₂ (balloon), phosphate buffer (pH 7), MeOH, rt, 2 d. (f) SO₃-Et₃N, DMF, 60 °C, 3 d. (g) TBAF, THF, 60 °C. (h) SO₃-Pyr, H₂O (adjusted to pH 9.5 by NaOH_(aq)), rt.

HS offers multiple epitopes to FGFs, and oligomerization is not uncommon along the sugar chain. HS acts as storage reservoir for FGFs, thereby increasing their local concentration and, at the same time, protecting the protein from degradation. At the cell surface, HS mediates the interaction of FGF with its receptor (FGFR), which also carries an HS-binding region, and stabilizes the 2:2 FGF:FGFR dimer that is a known prerequisite for full range signaling.¹⁷ The differences in HS-binding specificity among the 18 known mammalian FGFs arise from their variable N- and C-terminal regions. Previous studies on FGF-1, in particular, suggested a sequence containing the N- and 6-O-sulfonated GlcN and 2-O-sulfonated IdoA as FGF-1 binding site,¹⁸ while the minimal sugar length remains in contention.¹⁹

To elucidate the structural features recognized by FGF-1 in natural HS, we screened the binding specificity of FGF-1 with our 48 HS-based disaccharides using isothermal titration calorimetry (ITC). Here, the protein solution in Tris-buffered

saline (pH 7.6) was titrated with the sugar dissolved in the same buffer at 25 °C. The heat of dilution was accounted for by the sugar titration of a separate blank solution. For the purpose of comparison, we also measured the FGF-1-binding affinity of a commercially acquired 3 kDa heparin. This material is a mixture of oligosaccharides averaging around 9 sugar units, with the N- and 6-O-sulfonated GlcN and 2-O-sulfonated IdoA as major components. ITC measurements showed that FGF-1 associated only with sugars **89–92** exhibiting dissociation constants (K_D) ranging from 4.1 to 21.2 μ M (Table 1). Affinity

Table 1. Dissociation Constants of the Sugars that Bind to FGF-1 Determined Through ITC^a

entry	sugar	K_D (μ M)
1	89	18.1
2	90	4.13
3	91	21.2
4	92	9.71
5	3 kDa heparin	0.746

^aMeasured as association constant, the inverse of K_D .

with FGF-1 is strongest for compound **90** among the disaccharides, which is about 5-fold lower than 3 kDa heparin. Conversely, the disaccharide incorporating the major heparin sugar units, compound **91**, displayed a 5-fold lower affinity than **90**. Common distinctive features of the binding disaccharides are the GlcN N-sulfonate and the IdoA 2-O-sulfonate moieties alluding to their critical roles in FGF-1 binding. The affinity enhancement observed in the presence of the 3'-O-sulfonate, but not with the 6'-O-sulfonate group, is indicative of the contribution these groups provide during the encounter.

We next examined the molecular details of the complex formation between the protein and the disaccharides. The four identified sugars were separately cocrystallized with FGF-1 and then subjected to X-ray analyses. The cocrystal structures were solved and refined to 2.80, 2.37, 2.34, and 2.50 Å resolutions for the respective protein complexes with compounds **89–92** (Figure 2). Together with the ITC data, these results defined the shortest HS-based compounds that bind to FGF-1. The disaccharides made identical contacts with the protein as anticipated from their many structural similarities (Table 2). The mutual binding site is formed by Asn18, Lys113, Lys118, Gln127, and Lys128—part of those that associated with longer HS oligosaccharides²⁰ and sucrose octasulfate²¹ in previous studies. Examinations of the crystal structures with longer HS oligosaccharides do not preclude the possible binding of our disaccharides in adjacent regions of the protein with another set of amino acid residues. Because we did not observe this scenario, it could be surmised that the five residues in the mutual binding site are the primary contact points in FGF-1 binding with natural HS. Moreover, the protein binding pocket occupied by our disaccharides and shared with longer HS oligosaccharides in previous reports²⁰ is shallow and relatively unhindered, warranting the extrapolation of disaccharides as HS substitutes in defining specificity. Most interactions involved the N-sulfonate of GlcN and the 2-O-sulfonate of IdoA as hinted by the ITC results. Notably, the 3-hydroxyl of IdoA has apparent H-bonding with Asn18 and Lys113. Also consistent with the ITC data, the 3'-O-sulfonate group in the disaccharides **90** and **92** exhibited electrostatic interaction with the side chain of Lys118, further strengthening the binding affinity. On the other hand, the 6'-O-sulfonate and the

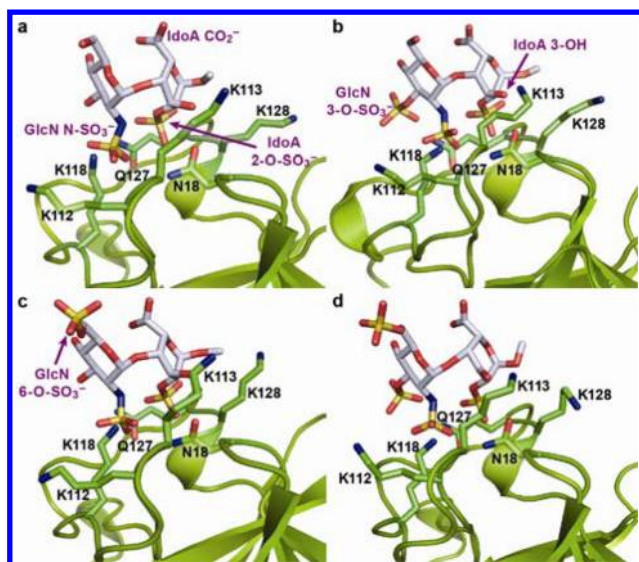


Figure 2. FGF-1 complexed with disaccharides (a) **89** (PDB code 3ud7), (b) **90** (PDB code 3ud8), (c) **91** (PDB code 3ud9), and (d) **92** (PDB code 3uda). Colors red, yellow, and blue represent oxygen, sulfur, and nitrogen atoms, respectively.

Table 2. Potential Intermolecular Interactions Within the FGF-1–Disaccharide Interface

FGF-1 residue (atom)	sugar group or atom (residue)	distance (Å)			
		89	90	91	92
Asn18 (Nδ2)	2-O-SO ₃ ⁻ (IdoA)	3.7	3.8	3.4	3.4
	2-N-SO ₃ ⁻ (GlcN)	3.5	2.8	3.1	2.9
Asn18 (Oδ1)	3-OH (IdoA)	2.9	3.0	3.1	3.3
Lys113 (NH)	2-N-SO ₃ ⁻ (GlcN)	3.0	2.7	2.6	3.1
Lys113 (Nζ)	3-OH (IdoA)	3.5	2.4	3.4	2.5
Lys118 (Nζ)	2-O-SO ₃ ⁻ (IdoA)	3.9	3.6	3.0	3.7
	2-N-SO ₃ ⁻ (GlcN)	2.8	2.7	2.6	3.3
Gln127 (Ne2)	3-O-SO ₃ ⁻ (GlcN)	–	3.0	–	3.4
	2-O-SO ₃ ⁻ (IdoA)	2.9	3.8	3.8	4.0
Lys128 (NH)	2-O-SO ₃ ⁻ (IdoA)	3.0	2.9	2.9	2.7

carboxylate groups made no contacts with FGF-1. Their outward orientations in our crystal structures suggest potential roles in the interface between HS and FGFR or perhaps in minor interaction with another FGF-1 in the active complex. Thus, the FGF-1–FGFR interaction may be suppressed by removing these nonparticipating moieties, and by the same token, compound **90** could potentially act as inhibitor of FGF-1 activity. FGF dimerization was previously observed with longer HS-based oligosaccharides¹⁷ and sucrose octasulfate²¹ but is unlikely in our case. Instead, as HS assumes a repeating tetrasaccharide helical structure,²² two FGF-1s could possibly bind, in *trans*-orientation, at the adjacent N-sulfonated GlcN and 2-O-sulfonated IdoA sequences (i.e., GlcN–IdoA–GlcN–IdoA) to form an HS-bridged FGF-1 dimer. Under such arrangement, the 6-O-sulfonate group, if available in the internal GlcN, may likely strengthen the dimerization by further interaction with the other FGF-1.

CONCLUSIONS

We have demonstrated an effective divergent strategy that provided efficient access to a comprehensive HS-based disaccharide library. Our orthogonal protecting group combi-

nations together with various transformation schemes may serve as a model in creating sets of longer HS-based constructs in the future. The availability of 48 HS-based disaccharides permitted the clarification of the different HS structures that can participate in FGF-1 binding as well as the specific major and minor interactions involved. Future evaluations with longer HS-based libraries may further identify subtle yet noteworthy binding details. Hence, as glycans hold immense importance in nature, so do diverse libraries of synthetic sugars in elucidating the molecular mechanisms and specificities of glycan–ligand interactions.

EXPERIMENTAL SECTION

Chemical Synthesis. The complete experimental details and compound characterization data can be found in the SI.

Protein Expression and Purification. The human FGF-1 gene was cloned in pET-21a expression vectors and transformed into the BL21 (DE3) strains cultured in lysogeny broth supplemented with 100 μg·mL⁻¹ ampicillin. Protein expression was induced with 1.0 mM isopropyl-1-thio-β-D-galactoside at 37 °C for 4 h. The crude cell extracts were loaded onto a heparin affinity column followed by gel filtration (Superdex 200, Pharmacia) of the FGF-1-containing fractions. The purified proteins were dialyzed against Tris-buffered saline (pH 7.6) and concentrated to levels suitable for ITC and cocrystallization. Protein concentrations were measured by typical UV and optical density analysis.

ITC Measurements. All ITC experiments were carried out at 25 °C using Tris buffer (20 mM Tris, 100 mM NaCl, pH 7.6) as solvent. The sugars (0.43–0.92 mg) were dissolved in Tris buffer to the desired concentrations (Figure S1). The FGF-1 solution was placed in the calorimeter cell and titrated with the sugar solution (2 μL injections with 3 min spacing). To account for the heat of the dilution, the buffer without the protein was also titrated with the sugar solution, and the generated data were subtracted from the results of the protein titration. The titration isotherms were fitted to an equation modeling the interaction (One Sites) to generate the fitting parameters.

Crystallization and Data Collection. FGF-1 (10 mg·mL⁻¹ in Tris-buffered saline) was separately mixed with disaccharides **89–92** in 1:1.2 molar ratio. All crystals were grown by hanging drop vapor diffusion at rt by mixing 1 μL of protein complex solution with 1 μL of reservoir solution containing 2 M (NH₄)₂HPO₄ and 0.1 M sodium acetate at pH 7.0. Diffraction data were collected at –150 °C at beamline 13B1 of the National Synchrotron Radiation Research Center in Hsinchu, Taiwan, and were processed and scaled by HKL2000.²³

Structure Determination and Refinement. The FGF-1–disaccharide complexes all crystallized in the C2 space group with three molecules per asymmetric unit. The structures were solved by molecular replacement using the crystal structure of FGF-1 (PDB code 1rg8) as the searching model. The structural model was subjected to manual rebuilding with WinCoot²⁴ and then refined using REFMAC5.²⁵ The data collection and refinement statistics are available in Table S1.

ASSOCIATED CONTENT

Supporting Information

Figure S1, Table S1, synthetic methods and characterization data, and ¹H and ¹³C NMR spectra of relevant compounds. This material is available free of charge via the Internet at <http://pubs.acs.org>.

AUTHOR INFORMATION

Corresponding Author

schung@gate.sinica.edu.tw

Author Contributions

[#]These authors contributed equally.

Notes

The authors declare no competing financial interest.

ACKNOWLEDGMENTS

This work was supported by the National Science Council (NSC 97-2113-M-001-033-MY3, NSC 98-2119-M-001-008-MY2, 100-2113-M-001-019-MY3) and Academia Sinica.

REFERENCES

- (1) Schmaltz, R. M.; Hanson, S. R.; Wong, C.-H. *Chem. Rev.* **2011**, *111*, 4259–4307.
- (2) (a) Capila, I.; Linhardt, R. J. *Angew. Chem., Int. Ed.* **2002**, *41*, 390–412. (b) Bishop, J. R.; Schuksz, M.; Esko, J. D. *Nature* **2007**, *446*, 1030–1037.
- (3) Esko, J. D.; Selleck, S. B. *Annu. Rev. Biochem.* **2002**, *71*, 435–471.
- (4) Gandhi, N. S.; Mancera, R. L. *Chem. Biol. Drug Res.* **2008**, *72*, 455–482.
- (5) Petitou, M.; van Boeckel, C. A. A. *Angew. Chem., Int. Ed.* **2004**, *43*, 3118–3133.
- (6) (a) Zhu, X.; Schmidt, R. R. *Angew. Chem., Int. Ed.* **2009**, *48*, 1900–1934. (b) Hsu, C.-H.; Hung, S.-C.; Wu, C.-Y.; Wong, C.-H. *Angew. Chem., Int. Ed.* **2011**, *50*, 11872–11923.
- (7) Dulaney, S. B.; Huang, X. In *Advances in Carbohydrate Chemistry and Biochemistry*; Derek, H., Ed.; Elsevier: Amsterdam, 2012; Vol. 67, pp 95–136.
- (8) (a) Peterson, S.; Frick, A.; Liu, J. *Nat. Prod. Rep.* **2009**, *26*, 610–627. (b) Liu, R.; Xu, Y.; Chen, M.; Weiwer, M.; Zhou, X.; Bridges, A. S.; DeAngelis, P. L.; Zhang, Q.; Linhardt, R. J.; Liu, J. *J. Biol. Chem.* **2010**, *285*, 34240–34249. (c) Xu, Y.; Masuko, S.; Takiuddin, M.; Xu, H.; Liu, R.; Jing, J.; Mousa, S. A.; Linhardt, R. J.; Liu, J. *Science* **2011**, *334*, 498–501.
- (9) (a) de Paz, J. L.; Martín-Lomas, M. *Eur. J. Org. Chem.* **2005**, 1849–1858. (b) Noti, C.; de Paz, J. L.; Polito, L.; Seeberger, P. H. *Chem.—Eur. J.* **2006**, *12*, 8664–8686. (c) Baleux, F.; Loureiro-Morais, L.; Hersant, Y.; Clayette, P.; Arenzana-Seisdedos, F.; Bonnaffé, D.; Lortat-Jacob, H. *Nat. Chem. Biol.* **2009**, *5*, 743–748. (d) Arungundram, S.; Al-Mafraji, K.; Asong, J.; Leach, F. E., III; Amster, I. J.; Venot, A.; Turnbull, J. E.; Boons, G.-J. *J. Am. Chem. Soc.* **2009**, *131*, 17394–17405. (e) Wang, Z.; Xu, Y.; Yang, B.; Tiruchinapally, G.; Sun, B.; Liu, R.; Dulaney, S.; Liu, J.; Huang, X. *Chem.—Eur. J.* **2010**, *16*, 8365–8375. (f) Hu, Y.-P.; Lin, S.-Y.; Huang, C.-Y.; Zulueta, M. M. L.; Liu, J.-Y.; Chang, W.; Hung, S.-C. *Nat. Chem.* **2011**, *3*, 557–563. (g) Hung, S.-C.; Lu, X.-A.; Lee, J.-C.; Chang, M. D.-T.; Fang, S.-I.; Fan, T.-c.; Zulueta, M. M. L.; Zhong, Y.-Q. *Org. Biomol. Chem.* **2012**, *10*, 760–772. (h) Zulueta, M. M. L.; Lin, S.-Y.; Lin, Y.-T.; Huang, C.-J.; Wang, C.-C.; Ku, C.-C.; Shi, Z.; Chyan, C.-L.; Irene, D.; Lim, L.-H.; Tsai, T.-I.; Hu, Y.-P.; Arco, S. D.; Wong, C.-H.; Hung, S.-C. *J. Am. Chem. Soc.* **2012**, *134*, 8988–8995.
- (10) Chao, C.-S.; Yen, Y.-F.; Hung, W.-C.; Mong, K.-K. T. *Adv. Synth. Catal.* **2011**, *353*, 879–884.
- (11) (a) Wang, C.-C.; Lee, J.-C.; Luo, S.-Y.; Kulkarni, S. S.; Huang, Y.-W.; Lee, C.-C.; Chang, K.-L.; Hung, S.-C. *Nature* **2007**, *446*, 896–899. (b) Wang, C.-C.; Kulkarni, S. S.; Lee, J.-C.; Luo, S.-Y.; Hung, S.-C. *Nat. Protoc.* **2008**, *3*, 97–113. (c) Chang, K.-L.; Zulueta, M. M. L.; Lu, X.-A.; Zhong, Y.-Q.; Hung, S.-C. *J. Org. Chem.* **2010**, *75*, 7424–7427.
- (12) Xu, Y.-C.; Bizuneh, A.; Walker, C. *Tetrahedron Lett.* **1996**, *37*, 455–458.
- (13) Kulkarni, S. S.; Hung, S.-C. *Lett. Org. Chem.* **2005**, *2*, 670–677.
- (14) Shangquan, N.; Katukojvala, S.; Greenberg, R.; Williams, L. J. *J. Am. Chem. Soc.* **2003**, *125*, 7754–7755.
- (15) Scheidt, K. A.; Chen, H.; Follows, B. C.; Chemler, S. R.; Coffey, D. S.; Roush, W. R. *J. Org. Chem.* **1998**, *63*, 6436–6437.
- (16) (a) Beenken, A.; Mohammadi, M. *Nat. Rev. Drug Discovery* **2009**, *8*, 235–253. (b) Turner, N.; Grose, R. *Nat. Rev. Cancer* **2010**, *10*, 116–129.
- (17) Mohammadi, M.; Olsen, S. K.; Goetz, R. A. *Curr. Opin. Struct. Biol.* **2005**, *15*, 506–516.
- (18) Harmer, N. J. *Biochem. Soc. Trans.* **2006**, *34*, 442–445.
- (19) Wu, Z. L.; Zhang, L.; Yabe, T.; Kuberan, B.; Beeler, D. L.; Love, A.; Rosenberg, R. D. *J. Biol. Chem.* **2003**, *278*, 17121–17129.
- (20) (a) DiGabriele, A. D.; Lax, I.; Chen, D. I.; Svahn, C. M.; Jaye, M.; Schlessinger, J.; Hendrickson, W. A. *Nature* **1998**, *393*, 812–817. (b) Canales, A.; Lozano, R.; López-Méndez, B.; Angulo, J.; Ojeda, R.; Nieto, P. M.; Martín-Lomas, M.; Giménez-Gallego, G.; Jiménez-Barbero, J. *FEBS J.* **2006**, *273*, 4716–4727.
- (21) Kulahin, N.; Kiselyov, V.; Kochoyan, A.; Kristensen, O.; Kastrup, J. S.; Berezin, V.; Bock, E.; Gajhede, M. *Acta Crystallogr.* **2008**, *F64*, 448–452.
- (22) Rabenstein, D. L. *Nat. Prod. Rep.* **2002**, *19*, 312–331.
- (23) Otwinowski, Z.; Minor, W. *Methods Enzymol.* **1997**, *276*, 307–326.
- (24) Emsley, P.; Cowtan, K. *Acta Crystallogr.* **2004**, *D60*, 2126–2132.
- (25) Collaborative Computational Project, Number 4; *Acta Crystallogr.* **1994**, *D50*, 760–763.